Structure and dynamics of two-dimensional lattices in random pinning potentials

Zhi-Xiong Cai
Materials Science Division, Brookhaven National Laboratory, Upton, New York 11973

Surajit Sen
Department of Physics, State University of New York at Buffalo, Buffalo, New York 14260

David O. Welch
Materials Science Division, Brookhaven National Laboratory, Upton, New York 11973

(Received 13 September 1994)

Two-dimensional lattices in random potentials characterized by weakly attractive random pinning sites were studied via molecular-dynamics simulations. For a sufficiently high density of pinning sites, a "fragile" glasslike (i.e., amorphous solid) phase is found to be stable at temperatures slightly below the melting temperature. Simulations suggest that this phase can be replaced by a more stable phase, namely, an approximately long-range-ordered solid phase, as the pins are made less dense and/or with weaker strength. The dynamics of the system depends sensitively on the density of pinning sites. This is probed by studying the velocity autocorrelation function of the particles in a random pinning potential as a function of the density of pinning sites.

I. INTRODUCTION

Two-dimensional lattices in random pinning potentials are realized in a variety of circumstances. The most common examples in physical systems include solid films with quenched impurities and/or on rough substrates[1–5] and flux-line lattices in type-II superconductive films.[6–12] The study of the equilibrium properties of two-dimensional lattices (i.e., without substrate potentials) in the melting region[13–16] is still an active research area.[17] The study of the effects of a uniform substrate corrugation on the structural properties of two-dimensional lattices, as found, for example, in high-stage alkali graphite intercalation compounds[18–27] and in adatoms on surfaces, continues to be an area of strong current interest.[28] At present, however, very little appears to be known about the structural properties of two-dimensional lattices in random potentials,[29] and in general, very little appears to be known about the dynamical properties of all of these systems.[30–33] This paper concerns the structural and dynamical properties of two-dimensional lattices in random pinning potentials. The underlying similarities between this problem and the well-known problem of the pinning of flux-line lattices in type-II superconductors have been addressed recently in Ref. 34.

Two key issues are studied in this work. First, the structural properties of the lattices as characterized in terms of sites with fivefold and sevenfold coordinations or defect pairs[12,13] in the solid phase near the melting transition as the density of pinning sites is varied. Second, the dynamical properties are measured via the velocity autocorrelation function of representative particles in the system in the same temperature regime under the same parametric variation.

The paper is organized as follows. Section II describes the model, the parameters chosen for the molecular dynamics studies, and the details of the simulation procedure. The results are discussed in Sec. III. Section IV summarizes this work.

II. MODEL SYSTEM AND THE SIMULATIONS

The interaction energy of the N-particle system with N_p randomly distributed pinning sites is defined as

$$V = \sum_{i,j=1(i\neq j)}^{N} V_2(|\mathbf{r_i} - \mathbf{r_j}|) + \sum_{i=1}^{N}\sum_{p=1}^{N_p} V_p(|\mathbf{r_i} - \mathbf{r_p}|), \tag{1}$$

which consists of both one- and two-body interactions. The two-body interaction potential between the particles is chosen to be similar to that between alkali metal ions in graphite intercalation compounds (see, for example, Refs. 19–21 where some details concerning this potential are presented). The two particles, each with with charge q and at distance $r_{ij} \equiv |\mathbf{r_i} - \mathbf{r_j}|$ apart, interact with an energy given by

$$V_2(r_{ij}) = \frac{q^2}{r_{ij}} \exp\{-r_{ij}/\lambda\}, \tag{2}$$

where q^2=4.8028$\times 10^{-10}$ esu and λ = 2.1 Å is the screening length. The one-body pinning potential is assumed to consist of a random distribution of attractive Gaussian potential wells, whose function form V_p is given by

$$V_p = -\frac{A_p}{2\pi} \exp[-(|\mathbf{r_i} - \mathbf{r_p}|)^2/R_p^2], \tag{3}$$

where A_p was chosen to be either 5 or 10 in the chosen energy unit which was $300k_B$ (k_B=Boltzmann constant) and which represents the strength of the pinning center (we have also studied the model for weaker and stronger A_p's which suggested the present choice of magnitudes of A_p), R_p represents the width of the pins and is chosen to be a unit length a_0 which was kept as 2.46 Å (for purposes of comparison with previous works in Refs. 24–27), and $\mathbf{r_p}$ is the location of the center of the pth pin. The pinning centers are distributed randomly within the simulation cell. Periodic boundary conditions are utilized in all of the simulations. The presence of pinning centers has a considerable effect on the structure and dynamics of our system. We have fixed the area of the molecular-dynamics (MD) supercell; thus by varying the number of pins, N_p, we can vary the density of the pins. The pinning density N_p per supercell and the strength A_p are the parameters of utmost interest in this study. As will be shown in Sec. III, it may be possible for a long-range-ordered solid to exist below the melting temperature for sufficiently small A_p in spite of large N_p. The system tends to be structurally very different when A_p is made stronger in that it resembles an amorphous solid or "glasslike" phase below the melting temperature.

The functional form of V_p used in this work is similar to that used by Shi and Berlinsky in Ref. 29 who study the static properties of a two-dimensional lattice with short-range two-body interactions. The two-body potential V_2, however, is different in this study, where a screened Coulomb potential has been used as opposed to the shorter-range Gaussian potential that was used in Ref. 29. Given the nature of the two-body potential and the magnitudes of the pinning strength used in this study, the reader may note that our pinning energy scale is significantly weaker than the two-body interaction energy scale. In this respect, the present study differs from the work in Ref. 29 in which the pinning strength played a more dominant role. The regime with strong competition between pinning and the two-body interaction addressed in this work may be directly relevant to the flux-line lattice problem in type-II superconductors.[35]

The molecular-dynamics simulations were performed using the microcanonical $(E, V, N, \mathbf{P})$ ensemble, where $\mathbf{P}$ is the total linear momentum of the system.[36] The Newtonian equations of motion for the system were integrated forward in time using a fifth-order Gear predictor-corrector algorithm[37] and the center of mass of the system was zeroed in every integration step. The mass unit was set as 1 amu and the particles were assumed to have the mass of Rb ions which meant that our natural time unit was approximately 1 ps. The runs for which the results are reported here had $N = 256$ distributed in a $36a_0 \times 36a_0$ rhombic supercell (a_0=2.46 Å is the length unit) which is commensurate with the triangular lattice for the particle density we studied. We considered cases with N_p equaling 0, 20, 100, 200, and 400 per supercell. The time step used in the simulation was 0.006 ps. Based upon our experience with previous studies,[24–27] we believe that this was a sufficiently fine integration time step for reliable calculation of the structure and dynamics of the present system. Starting from randomly distributed particles and pinning sites, the system was first heated up to about $T = 400$ K and equilibrated. This temperature is well above the melting temperature $T_m \sim 200$ K.[22] The temperature was then reduced in steps of 50 K from 400 K to 250 K and thereafter in steps of 20 K down to $T = 50$ K by carefully scaling down the velocities and by equilibrating the systems for ~ 300 ps. Thus, for each temperature, 50 000 time steps/particle were used to equilibrate the system before calculating the thermal averages of various quantities by using the data from the next 100 000 time steps. Most of the calculations we report in this study have been carried out at $T \sim 180$ K.

In order to monitor the freezing transition, we calculated the translational diffusion coefficient D using the relation

$$D = \lim_{t\to\infty} \frac{1}{4t} \langle [\mathbf{r}(t) - \mathbf{r}(0)]^2 \rangle, \tag{4}$$

where the angular brackets imply time averages (and hence, via the ergodicity assumption,[38] ensemble averages).

The structure of the system near the melting transition can be characterized in terms of the number of defects in the simulation cell. To obtain this information, Voronoi constructions[39] were carried out and the number of topological defects was monitored as a function of temperature and as a function of N_p. In addition, the dependence of the number of topological defects on A_p at various temperatures was also explored. The structure was also characterized using the circularly averaged pair-distribution function $g(r)$ of the systems studied. This is defined as

$$g(r) = \frac{A}{N^2} \left\langle \sum_{i,j(i\neq j)} \delta(|\mathbf{r} - \mathbf{r_{ij}}|) \right\rangle, \tag{5}$$

where A is the area of the supercell and the angular brackets imply a time average.

The dynamical properties of the system can be studied by calculating various response functions such as the dynamic structure factor $S(\mathbf{k}, \omega)$. Given that the present goal is to probe the most basic properties of the chosen system we have therefore studied one of the most simple and fundamental dynamical response functions, namely, the velocity autocorrelation function which can be defined as

$$Z(t) = \frac{\langle \sum_i \mathbf{v}_i(t).\mathbf{v}_i(0) \rangle}{\langle \sum_i \mathbf{v}_i(0).\mathbf{v}_i(0) \rangle}. \tag{6}$$

The reader may note that the velocity autocorrelation function is simply related to the diffusion constant as $D = \frac{1}{2}\int_0^\infty ds Z(s)$ [see Eq. (4) above].

III. RESULTS

Figure 1(a) shows the temperature dependence of the diffusion coefficient D for a pinning density $N_p = 100$ per supercell with the pinning strength $A_p = 5$ (dashed curve) and $A_p = 10$ (solid curve). In this study, we define the solid phase as the phase with $D \sim 0$ and the

fluid phase as the one with $D > 0$. Our simulation results suggest that the two-dimensional lattice in a weaker random potential has a higher melting temperature than it does when the pinning is strengthened, although this effect is difficult to quantify. The data in Fig. 1(a) reveal that the melting temperature for $A_p = 5$ is $T_m \approx 220$ K, whereas for $A_p = 10$, 180 K $\leq T_m \leq$ 200 K. The decrease in D in Fig. 1(a) as the temperature is raised between $T = 240$ K and $T = 250$ K is probably a fluctuation effect attributable to the rather small size of the system. Thus, the lattice with $A_p = 5$ behaves much like a two-dimensional lattice without pinning whereas the lattice with $A_p = 10$ appears to behave differently. To probe the real-space lattice structure of the two cases it is instructive to enumerate the number of topological defects (per supercell) in the lattice as a function of temperature for the two values of A_p under examination. This is shown in Fig. 1(b), where the dashed curve is for $A_p = 5$ and the solid curve is for $A_p = 10$. If we define a long-range-ordered solid as a system with the defect density $\delta \to 0$ (and $D \sim 0$) whereas a glassy system has $\delta > 0$ (and $D \sim 0$), the data in Fig. 1(b) strongly suggest that one obtains a glassy phase for $A_p = 10$ for $T < 200$ K or so. We prefer to call this phase a "fragile" glasslike phase because its emergence appears to be highly sensitive to the magnitude of A_p, at least, for the regime of N_p probed in this work. We shall now focus on the properties of this fragile glasslike phase itself.

Figure 2(a) shows the diffusion constant D as a function of temperature for $A_p = 10$ and varying pinning density $0 \leq N_p \leq 400$ [see the caption of Fig. 2(a) for details]. Observe that the diffusion coefficient for $A_p = 5$ and $N_p = 100$ in Fig. 1(a) is comparable to that for $N_p = 0$ case (i.e., a pure two-dimensional lattice case) in Fig. 2(a). The diffusion coefficient, however, behaves very differently as N_p is increased from 100 to 400. The system obviously becomes increasingly more "sluggish" as N_p is raised. Our data suggest that the melting temperature appears to increase slightly for $N_p \geq N$ compared to the $N_p < N$ case (the particle density N is 256 per supercell in all the calculations). Understanding the detailed dependence of T_m on N_p requires fur-

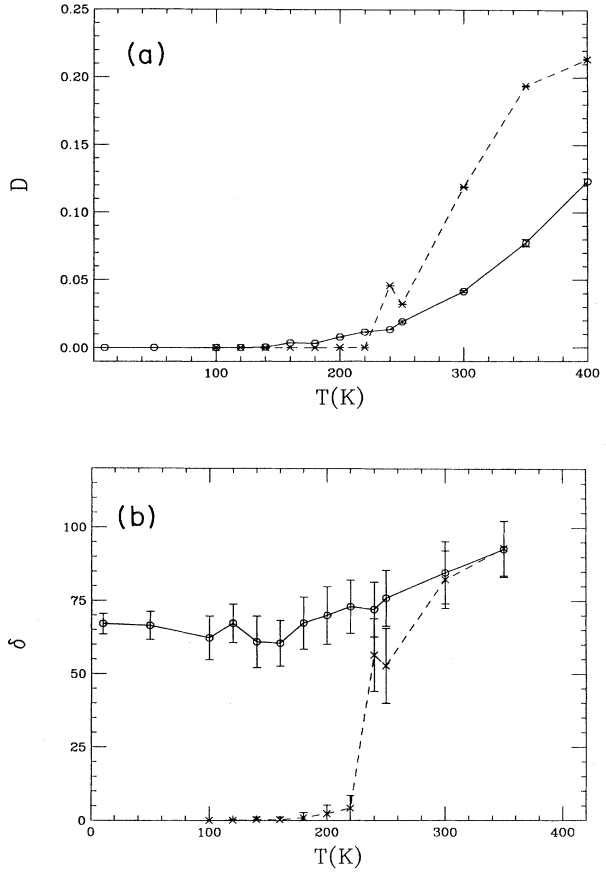

FIG. 1. (a) Temperature dependence of the diffusion coefficient D for a pinning density $N_p = 100$ per supercell with pinning strength $A_p = 5$ (dashed curve) and $A_p = 10$ (solid curve). (b) Number of topological defects per supercell as a function of temperature for a pinning density $N_p = 100$ per supercell with pinning strength $A_p = 5$ (dashed curve) and $A_p = 10$ (solid curve).

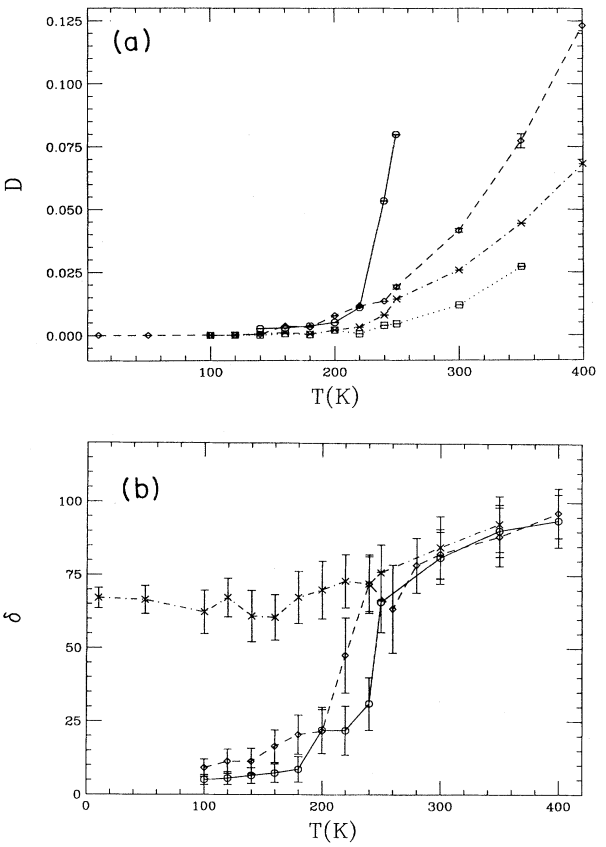

FIG. 2. (a) Temperature dependence of the diffusion coefficient D for various pinning densities N_p per supercell. ○, $N_p = 0$; ◇, $N_p = 100$; ×, $N_p = 200$; □, $N_p = 400$. (b) Temperature dependence of the number of topological defects per supercell for various pinning densities N_p per supercell. ○, $N_p = 0$; ◇, $N_p = 20$; ×, $N_p = 100$.

ther analysis, preferably using Monte Carlo techniques on very large systems, and will be addressed in a separate publication.[40]

As in Fig. 1(b), the number of defects as a function of temperature for various values of pinning density N_p's is shown in Fig. 2(b). Because of the large number of defects found in the solid phase (i.e., $D \sim 0$ phase) for $N_p \geq 100$ in our study, we only show the results for N_p =0, 20, 100. The data suggest that for $N_p \ll N$, $\delta \to 0$ for $T \ll T_m$ and hence the long-range-ordered solid phase emerges. Thus, the physical properties of the fragile glasslike phase depend sensitively on N_p and A_p. To summarize the results in Figs. 1 and 2, one may observe that the simulations suggest the existence of two different forms of solid phase characterized by $D \sim 0$. These are the ordered solid phase characterized by $\delta \sim 0$ and the fragile glass phase characterized by $\delta > 0$. In addition, the data suggest that T_m increases when $N_p > N$ for $A_p = 10$ and also as $A_p \to 0$.

Figure 3 shows the circularly averaged pair-distribution function $g(r)$ at $T = 180$ K for various densities of the pinning centers with pinning strength $A_p = 10$. The solid line refers to $N_p = 0$ and the peak positions reveal the existence of a triangular lattice. To see this, the reader may observe that the lattice constant for a 16×16 lattice on a $36a_0 \times 36a_0$ supercell is $a \equiv 2.25a_0$ (in units of $a_0 = 2.46$ Å), which is where the primary peak is located in Fig. 3. The second nearest neighbor is located at $\sqrt{3}a$, i.e., at $3.897a_0$, and the third nearest neighbor is at $2a = 4.5a_0$, while the fourth nearest neighbor is at $\sqrt{7}a = 5.953a_0$ and so on. The lattice is only slightly perturbed for small N_p, i.e., $N_p = 20$ (see dashed line in Fig. 3), a result which is in accordance with our observation using Fig. 2(b) above that the number of defects $\delta \to 0$ when $N_p \ll N$. The lattice structure, however, becomes drastically different as N_p is increased to 100 and higher. The $g(r)$ resembles that of a liquid[37] although the system possesses $D \sim 0$. This is the fragile glassy phase we have discussed earlier.

Figure 4 reveals information about the dynamics of a particle in the time domain. It reveals the motion of the particles on a microscopic time scale where dynamical details occurring over intervals of $\sim 10^{-13}$ s can be resolved. Since the interval is comparable to the typical time scale between particle collisions, one is effectively probing features of dynamical behavior most sensitive to the details of the interactions.

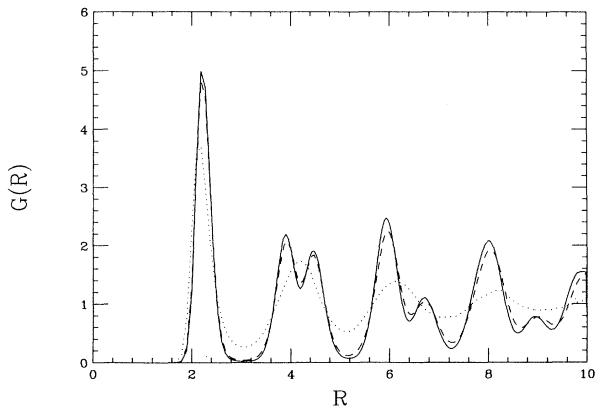

FIG. 3. The pair distribution functions at $T = 180$ K for various pinning densities N_p per supercell. Solid line, $N_p = 0$; dashed line, $N_p = 20$; dotted line, $N_p = 100$.

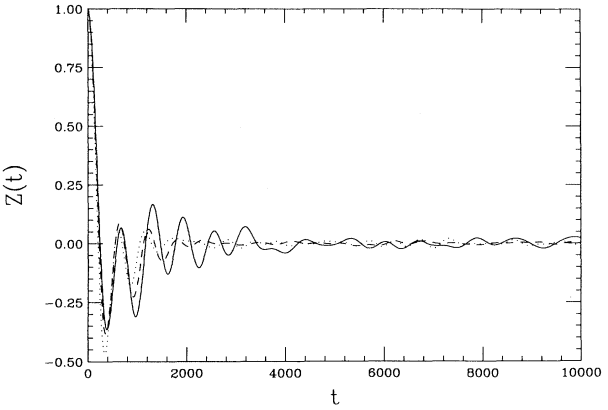

FIG. 4. The velocity autocorrelation functions at $T = 180$ K for various pinning densities N_p per supercell. Solid line, $N_p = 0$; dashed line, $N_p = 100$; dotted line, $N_p = 400$.

The short-time behavior of the velocity autocorrelation function can be studied by Taylor series expansion,[31] i.e.,

$$\mathbf{v}_i(t) = \mathbf{v}_i(0) + \mathbf{v}_i'(0)t + \frac{1}{2}\mathbf{v}_i''(0)t^2 + \cdots \quad . \tag{7}$$

Multiplying by $v_i(0)$ and taking an ensemble average we obtain

$$\begin{aligned}\langle \mathbf{v}_i(t) \cdot \mathbf{v}_i(0) \rangle &= \langle v_i^2 \rangle - \frac{1}{2}\langle v_i'^2 \rangle t^2 + \cdots \\ &= \langle v_i^2 \rangle \left(1 - \frac{1}{2}\Omega_0^2 t^2 + \cdots\right),\end{aligned} \tag{8}$$

where

$$\Omega_0^2 = \langle |F|^2 \rangle / 2mk_BT.$$

Time-reversal symmetry makes the odd terms in t vanish. The short-time behavior of the velocity autocorrelation function is related to the mean square acceleration (or mean square force $\langle |F^2| \rangle$) and provides information about the interaction between the particles, between the particles and the pins, and of the lattice structure of the system.

Figure 4 shows the velocity autocorrelation functions at $T = 180$ K for various densities of the pinning centers with pinning strength $A_p = 10$. For the pinning-free case, the particles form an ordered triangular lattice in the solid phase. A minimum in the velocity autocorrelation function occurs, indicating the correlations between the random force F and the velocity of any single particle in the system [see Eq. (8)]. A particle in the triangular lattice is trapped in the potential well due to the interaction with the other particles. With the presence of the pinning sites, the substrate "roughness" affects the motion of these particles in a significant way so that the Ω_0^2

increases, resulting in a faster decrease in the velocity autocorrelation function in the short-time regime.

The intermediate-time behavior of the velocity autocorrelation function is sensitive to the density of the pinning sites. The nature of the velocity autocorrelation function for the $N_p = 0$ case bears resemblance to that of a single particle in a strongly anharmonic corrugation potential.[32] As the pinning density is increased, the lattice becomes more disordered due to the random force field from these pinning sites. The memory effects (which produce correlations between random force and velocity) that cause the strong oscillations in the velocity autocorrelation function become less important for higher density of the pinning sites. This is evident from Fig. 4 in which the oscillatory behavior of the velocity autocorrelation function[41] undergoes strong attenuation as N_p is increased. The behavior of velocity autocorrelation function for the disordered system due to high pinning densities is different from the behavior of velocity autocorrelation function for the liquid phase[42] in spite of the fact that the structural similarities between the liquid phase and the fragile glassy phase are note worthy (see Figs. 2 and 3). Thus first minimum of the velocity autocorrelation function for the systems with high pinning densities is deeper compared to that in the ordered lattice and that in the liquid structure. This suggests that the interparticle forces are much stronger in the glassy phase at short ranges and hence very different dynamics should be expected.

IV. SUMMARY AND DISCUSSION

In summary, this study reports detailed molecular-dynamics simulations of two-dimensional lattices in a random pinning potentials, in particular a system which has screened-Coulomb interparticle interactions and weak pinning at temperatures that are slightly below the melting transition temperature.

We have calculated the diffusion coefficient D as a function of temperature for such two-dimensional lattices with a variable density of pins and for two different pinning strengths in the weak pinning regime. We found that there exists some characteristic pinning strength such that for relatively weak pins the effects of pinning are overcome by the particle-particle interactions. Thus, for sufficiently weak pinning, one observes a triangular lattice in the solid phase. This remains true even when the number of pins is comparable to the number of particles. The structure of the lattice, however, is drastically different and significantly disordered when the pinning strength is increased. The defect density increases the manifold in the lattice and the structural properties resemble that of a liquid (as in Fig. 3) in spite of a $D \sim 0$.

The microscopic dynamical properties of the system have been probed by studying the velocity autocorrelation function of a typical particle at $T \sim 180$ K. The calculations reveal that stronger pins lead to higher-frequency oscillations at the shortest time scales and attenuation at intermediate times in the velocity autocorrelation function when compared with the results of calculations on a pin-free two-dimensional lattice.

The study presented here is not system specific and hence can be useful in analyzing a variety of systems. Physical systems such as adatoms on solid surfaces[33] and flux-line lattices in type-II superconductors are examples of systems which offer closely related physical problems. Indeed, the nature of the glassy phase in type-II superconductors is an issue of much interest at the present time. Likewise, the structural and dynamical properties of films with quenched impurities[1] are being studied intensely by various groups. The present molecular-dynamics study is among the very few to probe the details of the structure and possibly the first to probe the dynamics of randomly pinned lattices in two dimensions.

ACKNOWLEDGMENTS

The authors are grateful to Professor A. John Berlinsky of McMaster University for inspiring them to undertake this work and for sharing many insights with them. They also wish to thank Dr. Normand Mousseau of the University of Oxford for his help in carrying out the constructions of the Voronoi polyhedra. Z.X.C. and D.O.W. would like to acknowledge support by the U.S. Department of Energy, Division of Materials Sciences, Office of Basic Energy Sciences under Contract No. DE-AC02-76CH00016. S.S. thanks the Physics Department of SUNY-Buffalo for support.

[1] C. Sagui and R.C. Desai, Phys. Rev. Lett. **71**, 3995 (1993).
[2] D.R. Nelson, Phys. Rev. B **27**, 2902 (1983).
[3] S. Sachdev and D.R. Nelson, J. Phys. C **17**, 5473 (1984).
[4] E.M. Chudnovsky, Phys. Rev. B **33**, 245 (1986).
[5] R.A. Serota, Phys. Rev. B **33**, 3403 (1986).
[6] A.I. Larkin, Zh. Eksp. Teor. Fiz. **58**, 1466 (1970) [Sov. Phys. JETP **31**, 784 (1979)].
[7] A.I. Larkin and Yu. N. Ovchinnikov, J. Low Temp. Phys. **34**, 409 (1979).
[8] B.A. Huberman and S. Doniach, Phys. Rev. Lett. **43**, 950 (1979).
[9] J.E. Fischer, Physica **99B**, 383 (1990).
[10] H.J. Jensen, A. Brass, and A.J. Berlinsky, Phys. Rev. Lett. **60**, 1676 (1988).
[11] A. Brass, H.J. Jensen, and A.J. Berlinsky, Phys. Rev. B **39**, 102 (1989).
[12] D.R. Nelson and V.M. Vinokur, Phys. Rev. B **48**, 13 060 (1993).
[13] B.I. Halperin and D.R. Nelson, Phys. Rev. B **19**, 2457 (1979).
[14] A.P. Young, Phys. Rev. B **19**, 1855 (1979).
[15] F.F. Abraham, Adv. Phys. **35**, 1 (1986).
[16] K.J. Strandburg, Rev. Mod. Phys. **60**, 161 (1988).
[17] See, for example, J.A. Zollweg and G.V. Chester, Phys. Rev. B **46**, R1186 (1992); K. Glasser, Ph.D. thesis, University of Colorado, 1991.

[18] *Graphite Intercalation Compounds*, edited by H. Zabel and S.A. Solin (Springer, Berlin, 1990), Vol. 1.
[19] M. Plischke and W.D. Leckie, Can. J. Phys. **60**, 1139 (1982).
[20] Z.M. Chen, O.A. Karim, and B.M. Pettitt, J. Chem. Phys. **89**, 1042 (1988).
[21] J.D. Fan, O.A. Karim, G. Reiter, and S.C. Moss, Phys. Rev. B **39**, 6111 (1988).
[22] J.D. Fan, Z.-X. Cai, G. Reiter, and S.C. Moss, Phys. Rev. B **48**, 1853 (1993).
[23] E. Vives and P.A. Lindgard, Phys. Rev. B **44**, 1318 (1991).
[24] H. Seong, S. Sen, T. Cagin, and S.D. Mahanti, Phys. Rev. B **45**, R8841 (1992).
[25] H. Seong, S. Sen, T. Cagin, and S.D. Mahanti, Phys. Rev. B **46**, 8748 (1992).
[26] T. Cagin, S. Sen, H. Seong, and S.D. Mahanti, Mol. Simulat. **10**, 41 (1993).
[27] J. Ellis and J.P. Toennies, Phys. Rev. Lett. **70**, 2118 (1993).
[28] A.C. Shi and A.J. Berlinsky, Phys. Rev. B **47**, 652 (1993).
[29] J.D. Fan, G. Reiter, and S.C. Moss, Phys. Rev. Lett. **64**, 188 (1990).
[30] H. Seong, Ph.D. thesis, Michigan State University, 1993.
[31] H. Seong and S.D. Mahanti, Phys. Rev. B **49**, 5042 (1994).
[32] L.Y. Chen and S.C. Ying, Phys. Rev. Lett. **71**, 4361 (1993).
[33] A.C. Shi and A.J. Berlinsky, Phys. Rev. Lett. **67**, 1926 (1991).
[34] J.E. Fischer, Physica **99B**, 383 (1990).
[35] Y. Zhu, Z.-X. Cai, R.C. Budhani, M. Suenaga, and D.O. Welch, Phys. Rev. B **48**, 6436 (1993).
[36] T. Cagin and J.R. Ray, Phys. Rev. A **37**, 247 (1988).
[37] M.P. Allen and D.J. Tildesley, *Computer Simulation of Liquids* (Clarendon, Oxford, 1987), Appendix E.
[38] For a recent discussion see S. Sen, Physica A **186**, 285 (1992).
[39] G.F. Voronoi, J. Reine Angew. Math. **134**, 198 (1908). See also, C.A. Rogers, *Packing and Covering* (Cambridge, New York, 1964).
[40] S. Sen and Z.-X. Cai (unpublished).
[41] S. Sen and S. Chakravarti, Physica A **209**, 410 (1994).
[42] J.-P. Boon and S. Yip, *Molecular Hydrodynamics* (McGraw-Hill, New York, 1980).